Magnetic and structural phase transitions of MnBi under high magnetic fields

2008 Sci. Technol. Adv. Mater. 9 024204

(http://iopscience.iop.org/1468-6996/9/2/024204)

Sci. Technol. Adv. Mater. **9** (2008) 024204 (5pp) doi:10.1088/1468-6996/9/2/024204

Magnetic and structural phase transitions of MnBi under high magnetic fields

Keiichi Koyama, Yoshifuru Mitsui and Kazuo Watanabe

High Field Laboratory for Superconducting Materials, Institute for Materials Research, Tohoku University, Sendai 980-8577, Japan

E-mail: kkoyama@imr.tohoku.ac.jp

Received 14 November 2007
Accepted for publication 9 January 2008
Published 20 May 2008
Online at stacks.iop.org/STAM/9/024204

Abstract

High-field x-ray diffraction and magnetization measurements and differential thermal analysis (DTA) were carried out for polycrystalline MnBi with an NiAs-type hexagonal structure to investigate its magnetic and structural phase transitions. The lattice parameter a rapidly decreases below the spin reorientation temperature $T_{SR}(= 90\,K)$ in a zero magnetic field. The parameter c decreases gradually with decreasing temperature and exhibits an anomaly in the vicinity of T_{SR}. By applying a magnetic field of 5 T, the parameter a increases by ~0.05% when $T < T_{SR}$ and varies smoothly when $8 \leqslant T \leqslant 300\,K$. DTA data show that the magnetic phase transition temperature from the ferromagnetic state to the paramagnetic state increases linearly at a rate of $2\,KT^{-1}$ with increasing magnetic field up to 14 T.

Keywords: MnBi, high-field x-ray diffraction, differential thermal analysis, high magnetic fields

1. Introduction

The intermetallic compound MnBi with an NiAs-type hexagonal structure (low-temperature phase: LTP) exhibits unique magnetic and structural properties [1–3]. The magnetic moment m of LTP can be extrapolated to a value of $3.9\,\mu_B\,Mn^{-1}$ at 0 K [4, 5]. With increasing temperature from room temperature (RT), LTP-MnBi undergoes a first-order magnetic phase transition from the ferromagnetic (FM) state to the paramagnetic (PM) state at $T_t \sim 630\,K$, accompanied by a structural transformation from the NiAs-type to a distorted Ni_2In-type hexagonal structure (high-temperature phase: HTP) [5]. The cell volume slightly decreases (<0.1%) in the transformation from LTP to HTP. Chen reported that HTP-MnBi is a separate compound with a chemical formula of $Mn_{1.08}Bi$ [6]. According to the Mn–Bi phase diagram [6], the phase transition of MnBi at T_t upon heating is associated with the peritectic decomposition of MnBi (LTP) into $Mn_{1.08}Bi$ (HTP) and liquid Bi. Recently, on the basis of magnetic measurements for MnBi, Liu *et al* [7] reported that T_t increases linearly with increasing magnetic field up to 10 T at a rate of $\sim 2\,KT^{-1}$. Differential thermal analysis (DTA) performed by Koyama *et al* [8] also showed an increase in T_t with increasing magnetic field at a rate of $2\,KT^{-1}$. In addition, they observed a metamagnetic phase transition between the PM state and a field-induced ferromagnetic (FFM) state in the vicinity of T_t [9]. These results suggest that the first-order phase transition with the peritectic composition and the decomposition of MnBi into $Mn_{1.08}Bi$ can be controlled by a magnetic field.

On the other hand, LTP-MnBi undergoes a spin reorientation transition at ~90 K. At RT, LTP-MnBi has uniaxial magnetic anisotropy along the c-axis [3]. The anisotropy constant decreases with decreasing temperature from RT, and becomes negative at ~90 K (T_{SR}) [3]. The magnetic moment lies in the c-plane below T_{SR}. This spin reorientation was also observed by neutron diffraction [10, 11] and nuclear magnetic resonance (NMR) [12] measurements on LTP-MnBi. However, the relation between the magnetic and structural properties has not yet been clarified in detail [10–13].

In this paper, we present the results obtained for the structural and magnetic properties of LTP-MnBi, which were investigated by measuring high-field x-ray diffraction at a low temperature, magnetization measurements and by DTA.

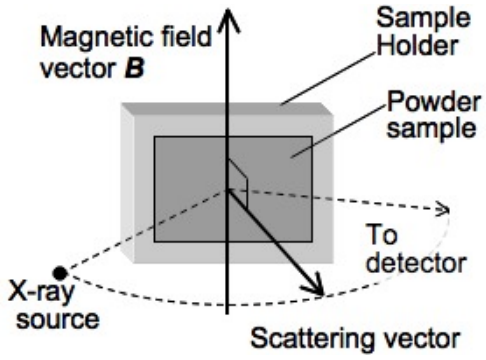

Figure 1. Schematic configuration of the powder sample and the x-ray beam path from the source to the detector. The powder sample is fixed using Apiezon grease on the copper holder in the cryostat. The x-ray scattering vector is perpendicular to the magnetic field vector.

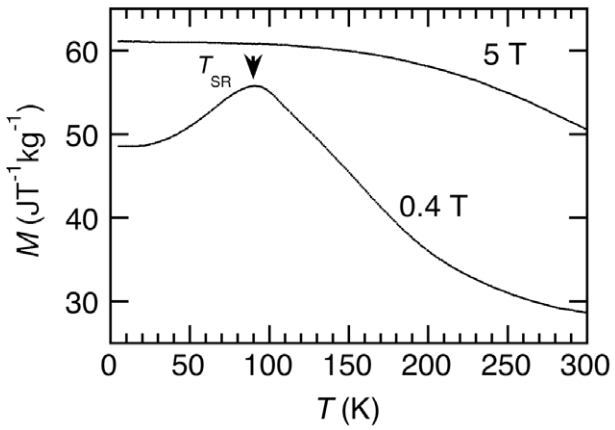

Figure 2. Temperature dependence of the magnetization of MnBi in magnetic fields of 0.4 and 5 T. The vertical arrow indicates the previously determined spin reorientation temperature T_{SR}.

2. Experimental

Polycrystalline MnBi was prepared by arc-melting a mixture of stoichiometric amounts of pure elements (Mn, 3N; Bi, 5N) in an argon atmosphere. The obtained button ingot was turned over and remelted several times. After that, the ingot was annealed at 573 K for 5 h in a quartz tube with an argon atmosphere and then quenched in water. X-ray powder diffraction measurements were carried out using CuKα radiation at RT. The sample was confirmed to be LTP-MnBi with small amounts of Bi and Mn, and we did not observe the reflection peaks of HTP-MnBi.

The magnetization M measurement was carried out below RT using a superconducting quantum interference device (SQUID) magnetometer. For $300 \leqslant T \leqslant 680$ K, M was measured using a Faraday force magnetometer in a magnetic field B of up to 10 T. The Faraday force magnetometer was described in [9] in detail. DTA was carried out under an argon atmosphere (ambient pressure) for $300 \leqslant T \leqslant 773$ K and $B \leqslant 14$ T. In this measurement, Al_2O_3 is utilized as a reference sample. A detailed description of high-field DTA can be found in [14].

High-field powder x-ray diffraction experiments were carried out using CuKα radiation at $8 \leqslant T \leqslant 300$ K using a Gifford-McMahon (GM) type cryocooler (helium gas closed-cycle refrigerator) and for $B \leqslant 5$ T using a cryocooled split-pair superconducting magnet [15]. The cryocooled superconducting magnet generates magnetic fields in the vertical direction. The x-ray scattering vector is in the horizontal direction (figure 1). A powder sample was fixed using Apiezon grease on a copper boat holder, which was attached to the second stage of the GM cryocooler in the cryostat. We confirmed that the powder sample was not removed by the magnetic force. The diffraction data were obtained for $20^\circ \leqslant 2\theta \leqslant 100^\circ$ with a step size of 0.01°.

3. Results and discussion

3.1. Magnetic and structural properties at low temperature

Figure 2 shows the temperature dependence of the magnetization (M–T curves) of MnBi at $B = 0.4$ and 5 T when $5 \leqslant T \leqslant 300$ K. For $B = 0.4$ T, we can see a cusp on the M–T curve at 90 K($= T_{SR}$), indicating that the spin reorientation occurs. For $B = 5$ T, the cusp was suppressed, and the magnetization decreases with increasing temperature. This result is consistent with a previous report [7]. Yoshida *et al* [13] observed thermal hysteresis in the temperature variation of the AC permeability of MnBi in the vicinity of T_{SR} and suggested that the spin reorientation transition is of the first order.

Figure 3(a) shows the powder x-ray diffraction patterns of LTP-MnBi at 292 K for $B = 0$ and 4 T. For $B = 4$ T, the 300 and 220 peaks are enhanced, though the *hkl* peaks are suppressed except for the 211 and 311 peaks. Because LTP-MnBi has uniaxial magnetic anisotropy along the c-axis at RT [3], most of the powder in the grease was aligned by the magnetic field, causing the enhancement of the 300 and 220 peaks. However, the 211 and 311 peaks are still observed, indicating that not all the powder was perfectly aligned by the magnetic field of 5 T. As shown in figure 3(a), the aligned powder remains even at a zero magnetic field. Subsequently, we carried out x-ray diffraction measurements under various temperatures and magnetic fields using this aligned sample. As examples of typical results, the powder x-ray diffraction patterns of MnBi at 8 K for $B = 0$ and 5 T are shown in figure 3(b). These results show that the aligned sample is fixed by the frozen grease at a low temperature. In this study, the lattice parameters a and c were determined using the 300 and 211 peaks.

Figure 4 shows the temperature dependences of the lattice parameters a (a) and c (b) and the cell volume V (c) of LTP-MnBi in a zero magnetic field. With decreasing temperature from 300 K, a decreases gradually. Upon further cooling, a decreases rapidly below 130 K ($= T_{SR1}$), and then it abruptly decreases below 90 K ($\sim T_{SR}$). When $T < T_{SR}$, a is almost constant. On the other hand, c and V decrease gradually with decreasing temperature and exhibit anomalies in the vicinity of T_{SR}. When $T < 60$ K, the parameter c is larger than immediately above T_{SR1}.

In our experimental configuration (figure 1), the enhanced 300 and 220 peaks are mainly due to the magnetically aligned

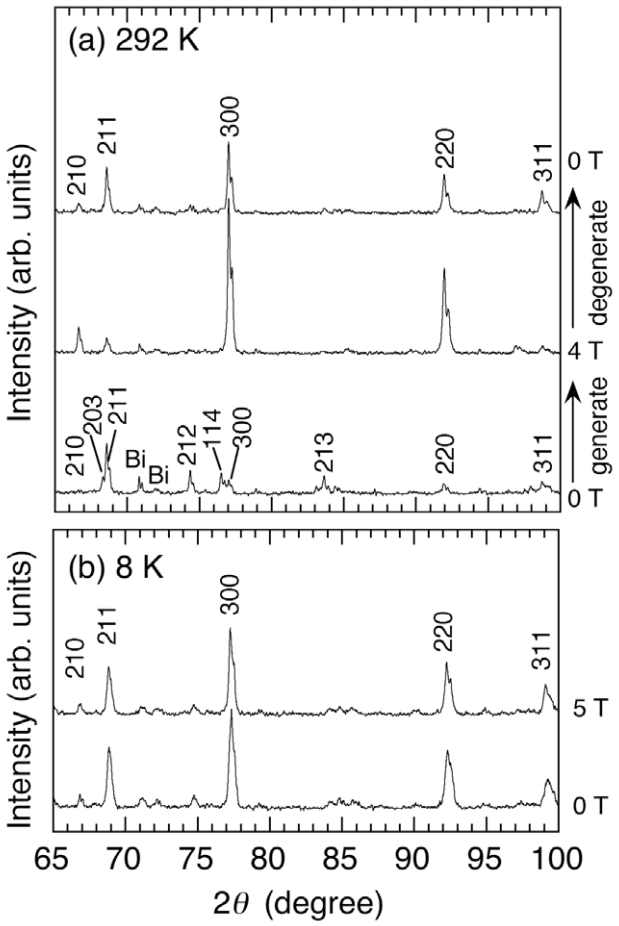

Figure 3. Powder x-ray diffraction patterns of MnBi in magnetic fields of 0 and 4 T at 292 K (a) and in magnetic fields of 0 and 5 T at 8 K (b).

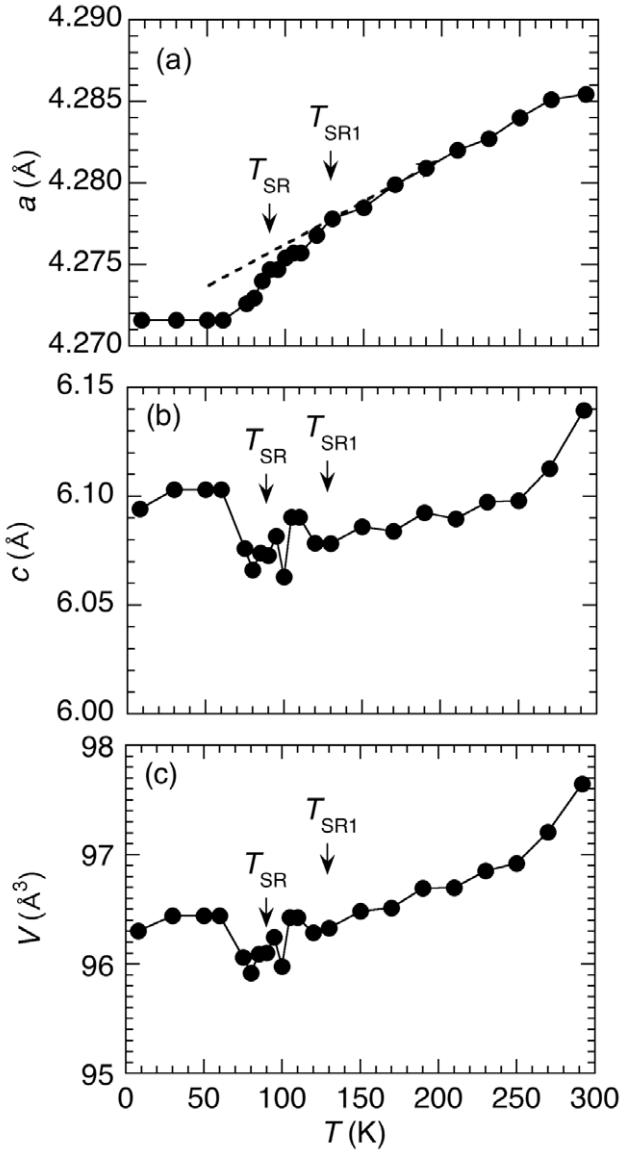

Figure 4. Temperature dependences of the lattice parameters a (a), c (b) and the cell volume V (c) of MnBi in a zero magnetic field. The vertical arrows indicate the characteristic temperatures of the spin reorientation T_{SR} and T_{SR1}. The broken line is a guide to the eyes.

powder, the c-axis of which is parallel to the magnetic field vector. On the other hand, the 211 and 311 peaks are mainly due to the misaligned powder. Therefore, we show the effect of only the magnetic field on the lattice parameter a by estimation from the position of the 300 peak. Figure 5 shows the temperature dependence of a for LTP-MnBi in a magnetic field of 5 T (open circles). Here, data obtained in a zero magnetic field (solid circles) are also illustrated for comparison. The rapid decrease in a when $T < T_{SR1}$ is recovered by applying a magnetic field of 5 T, and a expands by ~0.05% for $T < 70$ K.

The NMR measurements by Hihara and Kōi show that below 142 K the magnetic moment deviates gradually from the c-axis in LTP-MnBi and enters the c-plane at 90 K [12]. These characteristic temperatures are consistent with T_{SR1} (= 130 K) and T_{SR} (= 90 K). The rapid decrease in a when $T < T_{SR1}$ is due to the spin reorientation transition. When $T < T_{SR1}$, the magnetic moment rotates toward the c-axis upon applying a magnetic field of 5 T to the aligned powder fixed by frozen grease. This field-induced state is similar to the uniaxial state when $T > T_{SR1}$. Therefore, the lattice parameter a varies smoothly when $10 \leqslant T \leqslant 300$ K under a high magnetic field of 5 T. In this field-induced transition, the interaction between the magnetic field and the spin-orbit coupling probably plays an important role, as pointed out in previous reports [7, 11].

According to the report on the effect of pressure on LTP-MnBi by Yoshida *et al* [13], T_{SR} increases linearly with quasi-hydrostatic pressure P at the rate of $dT_{SR}/dP = 0.96\ \mathrm{K\,GPa^{-1}}$. They suggested that the cell volume in the state with the magnetic easy direction along the c-axis is larger than that when the axis is in the c-plane. However, it seems that the volume in both states is not greatly different. On the other hand, the magnetic properties of LTP-MnBi have been explained well by a mean field model with localized magnetic moments [8, 16], and the spin-orbit coupling affects the magnetic properties. Therefore, the ratio c/a in the crystal probably plays an important role in the spin reorientation. Measurements in high magnetic fields using an LTP-MnBi

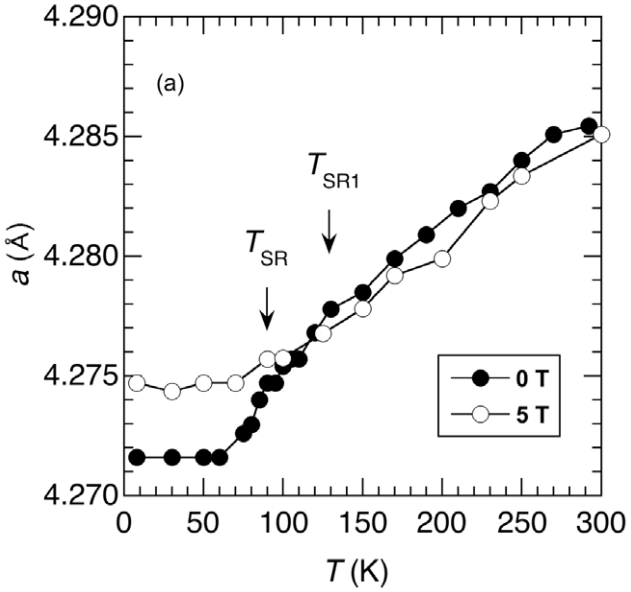

Figure 5. Temperature dependence of the lattice parameter a of MnBi in 5 T (open circles). The data in a zero magnetic field (solid circles) are also illustrated for comparison.

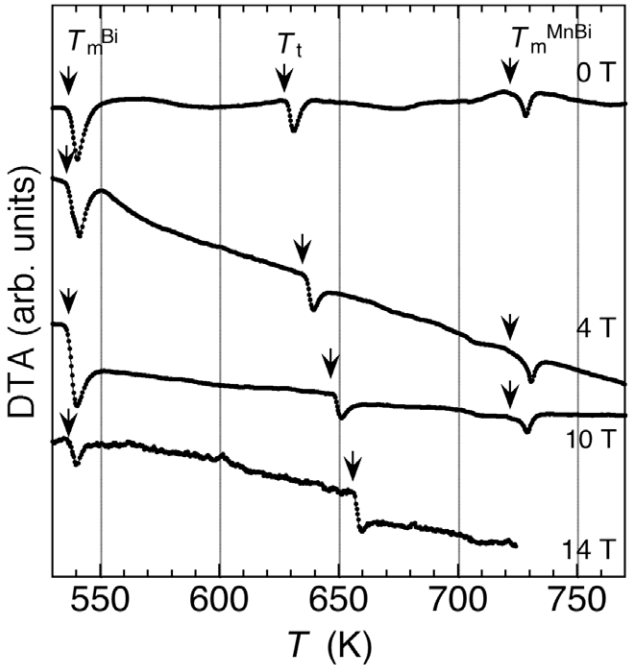

Figure 6. DTA curves for MnBi in various magnetic fields up to 14 T [8]. The data were obtained during heating. The vertical arrows indicate the previously determined phase transition temperatures.

single crystal are required for clarifying the magnetic and structural properties in detail.

3.2. Magnetic phase transition at high temperature

Figure 6 shows typical results for the DTA curves of MnBi for various B up to 14 T [8]. The data were obtained during heating at a rate of 3 K min^{-1}. For $B = 0$ T, three endothermic peaks were observed at $T_m^{Bi} = 533$ K (the melting point of Bi), $T_t = 628$ K (the phase transition from LTP to HTP) and $T_m^{MnBi} = 719$ K (the peritectic temperature of HTP). Here, these transition temperatures were determined by the onset of the endothermic peaks. Note that T_m^{Bi} and T_m^{MnBi} are independent of B, but T_t increases with increasing B.

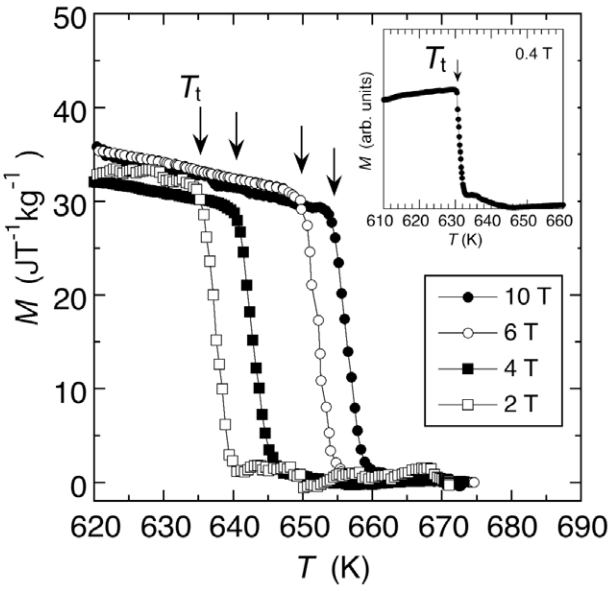

Figure 7. Temperature dependence of the magnetization of MnBi in various magnetic fields up to 10 T in the vicinity of the magnetic phase transition temperature, T_t [9]. The vertical arrows indicate the previously determined T_t.

Figure 7 shows typical results for the M–T curves in the vicinity of T_t [9]. Here, the data were also obtained during heating. In this figure, the vertical arrows indicate the previously determined magnetic phase transition temperatures. With increasing T, M abruptly vanishes at T_t even in higher magnetic fields, which indicates that the magnetic transition is of the first order. Liu *et al* [7] reported that the thermal hysteresis of T_t is about 10 K.

Figure 8 shows the magnetic field dependence of T_t for MnBi. Upon increasing B up to 14 T, T_t, as determined by DTA measurements, increases linearly by 2 KT^{-1}, although the data [9] obtained from the M–T curves are somewhat scattered. These results show that the endothermic peak at T_t in figure 6 is due to the first-order magnetic phase transition from the FM state to the PM state.

As shown in figure 6, the only single endothermic peak at T_t in the DTA data shifts to a higher temperature with increasing B, and no extra peak was observed in the vicinity of T_t. This suggests that the structural transformation during the peritectic decomposition is induced by the magnetic field and is accompanied by a first-order magnetic phase transition. That is, the magnetic field affects the first-order magnetic and structural transitions between FM-MnBi with the NiAs-type structure (LTP) and PM-$Mn_{1.08}Bi$ with the distorted Ni_2In-type structure (HTP). The transition at T_t probably occurs to minimize the magnetic and elastic energies between FM-LTP MnBi and PM-HTP $Mn_{1.08}Bi$. Upon applying a magnetic field to the compound, the decrease in the magnetic free energy of FM (FFM)-LTP MnBi is much

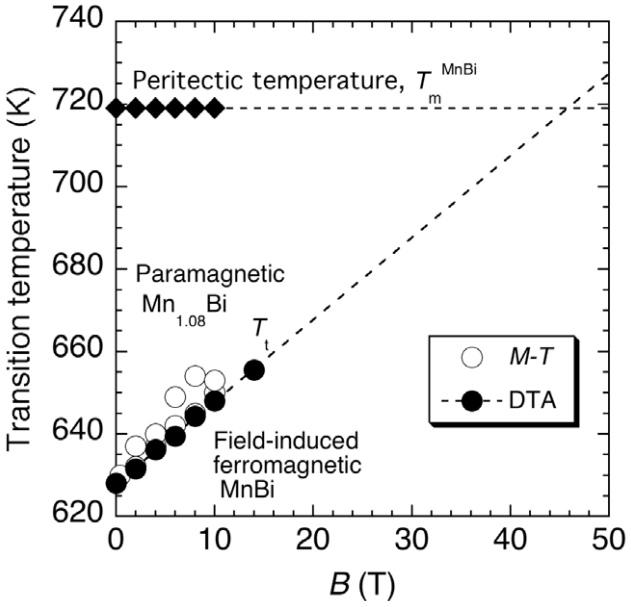

Figure 8. Magnetic phase diagram of MnBi. The solid and open circles indicate T_t determined by DTA [8] and the magnetic measurement [9] data, respectively. The solid diamonds indicate the peritectic temperature T_m^{MnBi} determined by the DTA data. The broken lines indicate the extrapolation calculated by the least-squares method for T_t and T_m^{MnBi} using the data determined by DTA.

larger than that of PM-HTP $Mn_{1.08}Bi$ because of the addition of the Zeeman energy. Therefore, we observe the increase in T_t by applying a magnetic field to this compound.

The mean field calculation shows that the Curie temperature T_C of LTP-MnBi is ~720 K [8, 16]. In addition, T_t linearly increases at a rate of 2–2.3 KT^{-1} in fields up to 14 T, as shown in figure 8. Assuming that this rate is constant at higher temperatures and in higher magnetic fields, T_t will reach the peritectic temperature ($T_m^{MnBi} \sim 720$ K) of HTP upon applying a magnetic field of ~45 T. Our mean field calculation suggested that the field-induced magnetic moment of LTP-MnBi is approximately $2\,\mu_B\,Mn^{-1}$ in a magnetic field of 45 T at 720 K [8]. This means that we may control the first-order magnetic and structural transitions of MnBi up to the peritectic temperature T_m^{MnBi} and solidify MnBi using a high magnetic field without inducing the PM phase. Therefore, from the point of view of magnetoscience, the control of the magnetic and structural properties and the chemical formula and the synthesis of the magnetic material MnBi under high magnetic fields are expected to be of considerable interest.

4. Summary

We carried out high-field x-ray diffraction and magnetization measurements and DTA for polycrystalline MnBi with the NiAs-type hexagonal structure. For $B = 0$ T, upon decreasing the temperature from room temperature, the lattice parameter a decreases rapidly below 140 K and is almost constant at temperatures below the spin reorientation temperature T_{SR} (= 90 K). The parameter c decreases gradually with decreasing temperature and exhibits an anomaly in the vicinity of T_{SR}. By applying a magnetic field of 5 T, the lattice parameter a increases by ~0.05% when $T < T_{SR}$ and varies smoothly when $10 \leqslant T \leqslant 300$ K. On the other hand, the magnetic phase transition temperature T_t from the ferromagnetic state to the paramagnetic state is 628 K in a zero magnetic field and linearly increases with field strength up to 14 T at a rate of 2 KT^{-1}. The obtained results suggest that we can control the unit cell dimensions for MnBi when $T < T_{SR}$, and its structural properties and chemical formula when $T > T_t$ by applying a high magnetic field.

Acknowledgments

The high-field x-ray diffraction, the magnetization measurement using the Faraday force magnetometer, and the high-field DTA experiments were carried out at the High Field Laboratory for Superconducting Materials, Institute for Materials Research, Tohoku University. The magnetization measurement using the SQUID magnetometer was performed at the Center for Low Temperature Science, Tohoku University. The authors are very much indebted to Dr H Yoshida for valuable discussions regarding the sample preparation. This work was partly supported by a Grant-in-Aid for Scientific Research from the Ministry of Education, Culture, Sports, Science and Technology, Japan, by the Iketani Science and Technology Foundation, and by the Nippon Sheet Glass Foundation for Materials Science and Engineering.

References

[1] Gullaud C 1951 *J. Phys. Radium* **12** 143
[2] Gullaud C 1951 *J. Phys. Radium* **12** 223
[3] Gullaud C 1951 *J. Phys. Radium* **12** 492
[4] Heikes R R 1955 *Phys. Rev.* **99** 446
[5] Roberts B W 1956 *Phys. Rev.* **104** 607
[6] Chen T 1974 *J. Appl. Phys.* **45** 2358
[7] Liu Y, Zhang J, Cao S, Jia G, Zhang X, Ren Z, Li X, Jing C and Deng K 2006 *Solid State Commun.* **138** 104
[8] Koyama K, Onogi T, Mitsui Y, Nakamori Y, Orimo S and Watanabe K 2007 *Mater. Trans.* **48** 2414
[9] Onogi T, Koyama K and Watanabe K 2007 *J. Japan. Inst. Met.* **71** 489 (in Japanese)
[10] Andersen A F, Hälg W, Fischer P and Stoll E 1967 *Acta Chem. Scan.* **21** 1543
[11] Yang J B, Yelon W B, James W J, Cai Q, Kornecki M, Roy S, Ali N and Ph l'Heritier 2002 *J. Phys.: Condens. Matter* **14** 6509
[12] Hihara T and Kōi Y 1970 *J. Phys. Soc. Japan.* **29** 343
[13] Yoshida H, Shima T, Takahashi T, Fujimori H, Abe S, Kaneko T, Kanomata T and Suzuki T 2001 *J. Alloys Compounds* **317** 297
[14] Awaji S, Watanabe K and Motokawa M 2001 *J. Cryst. Growth* **226** 83
[15] Watanabe K, Watanabe Y, Awaji S, Fujiwara M, Kobayashi N and Hasebe T 1998 *Adv. Cryog. Eng.* **44** 747
[16] Huberman B A and Streifer W 1975 *Phys. Rev.* B **12** 2741